EasyChair Preprint

№ 9465

Comparison of Mixed and Unmixed Turbofan Engine with Intake Air Cooling :Parametric Study and Optimization-TOPSIS Decision

Mohamad Sabzehali and Mahdi Alibeigi

December 12, 2022

Comparison of mixed and unmixed Turbofan engine with intake air cooling :Parametric Study and Optimization-TOPSIS Decision

M.Sabazeali, M. Alibeigi

Abstract

In this article, the effect of inlet air temperature on turbofan engines performance and optimization of turbofan engines performance in take off condition with inlet air cooling system is investigated. The objective functions are parameters that represent performance of the turbofan engine, are as follows thrust force, Specific fuel consumption (TSFC), thermal efficiency, nitrogen oxides emission index coefficient (snox) and turbine inlet temperature. Overall compressor pressure ratio, fan pressure ratio, and bypass ratio are considered as design variables. With inlet air temperature drop, thrust, TSFC, thermal efficiency, inlet air mass flow rate,fuel mass flow rate increase and snox decreases. Values of the performance parameters of the turbofan engine vary based on the optimization with four objective functions and hydrogen fuel to choose the optimal modes ,by defining weight coefficient and using the TOPSIS algorithm that have been selected for two environmental and economic approaches. For both engines with both approaches and using the decision-making method, the highest score and low score for optimization state belong to snox objective function and TSFC objective function, respectively. Thrust force of CFM56 3B2 and GENX 1B70 engines based on optimization with snox have increased by about 19.1% and 12.6%compared to the design.

Keywords: Fuel, inlet air cooling, environment-economic- thermo-economic, optimization, TOPSIS

Introduction

Nowadays, engine design is one of the most important stages of aircraft design besides engine designers are always trying to optimize the propulsion system. Aircraft designers and aircraft manufacturers have made many efforts in different fields such as structure design, aerodynamic design, etc.

Thermodynamic analysis of gas turbines is done to evaluate the performance of these engines and to optimize the thermodynamic cycle of gas turbines to find optimal values for cycle design variables. In this regard, Turan [1] investigated the effect of the Mach number on the energy and exergy performance of a small turbojet (TJ) engine as an unmanned drone aircraft. In Turan's study, the thermo - economic efficiency was investigated in terms of a constant flight of 8000 m (In Mach number of 3 to 0.8). the results showed that the Mach number between 0.3 to 0.8, the thermo - energy efficiency from 48.61 to 49.88, and the exergy efficiency of 3.25 % to 9.96 percent respectively. also, the Exergy efficiency has been evaluated for the centrifugal compressor, combustion chamber, and turbine as 61.11 %, 89.21 %,

and 84.11 % respectively. also, at a constant height, both the energy efficiency and exergy efficiency of the engine are increased by increasing the Mach number.

Najjar and Blawneh [2] investigated the thermodynamic performance of a small turbojet engine with a computer program of the General Algebraic Modeling System (GAMS). The effect of changes in flight Mach numbers from 0.3 to 0.9 and the changes in flight altitude from 3000 meters from sea level to 9000 meters from sea level was considered. The functioning constraints were compressor pressure ratio (*rp*) and turbine inlet temperature (*TIT*) where both of them have influenced the specific thrust (TSF) and specific fuel consumption (T*SFC*). Their results presented that the specific thrust powerfully depends on turbine inlet temperature (*TIT*), where a 10% reduction in *TIT* consequences reduced 6.7% TSFC and 6.8% in T*SFC*.

Seyam et al.[3] represented a unique hybrid-type aircraft propulsion system that syndicated with a civil turbofan system with a solid oxide fuel cell system (SOFC). Thermodynamic investigations and parametric studies were cooperatively executed to explore the compatibility and appropriateness of the considered system. Also, They analyzed the energetic and exergetic with different operating conditions. The alternative fuels included Hydrogen, methane, methanol, ethanol, and dimethyl ether with different combinations to substitute kerosene, which is an outmoded fossil-based fuel. They calculated the SOFC net power, electric efficiency, maximum thermal efficiency, exergetic efficiency with amounts of 944 kW, 87.0%, 32.3%, and 43.9% respectively. Also, the exergetic efficiency was accomplished by using methane and hydrogen fuel with amounts of 75% and 25% respectively.

Nordin et al.[4] analyzed the effect of compressor inlet air cooling on aero gas turbine engines and on performance of industrial gas turbine engines. They exposed that the aero-derivative gas turbine (GE LM6000PD) with turbine inlet air cooling technology produced more annual net energy output and higher net electrical efficiency rather than the industrial gas turbine.

In another study, Tang et al.[5] performed to evaluate the effect of airflow in High altitude low Reynolds number of turbofan engines. Their consequences indicated that under the Reynolds Numbers, the efficiency, the cross-air mass flow rate of rotary machine components have decreased.

In another study, V.Zare [6] studied the thermo-economy analysis and optimization with the objective function of a biomass-fueled gas turbine along with cooling air of compressor. in this study, an absorption refrigeration cycle for cooling air inlet air cooling is used. As a result, this study reduced the temperature of the incoming air to a 22.5 % decrease in the cost of electricity production.

Tuzcu et al.[7] executed the economic analysis of turbofan engines used in aircraft, Their result showed that the Energy efficiency of High-pressure turbines, low-pressure turbines, and combustion chambers is 19.7%, 26.2%, and 90% respectively.

Patel et al.[8] premeditated to optimize the efficiency, the specific fuel consumption, and Thrust force of a subsonic /supersonic turbojet engine. As a result, the optimization of the thermal efficiency and propulsive efficiency in the design point conditions were calculated by 70.95 and 60.23 %, respectively.

Najjar and Abubaker [9] explored analysis of the effect of inlet air cooling on gas turbine engines with heat recovery and exergitic optimization. The consequence indicated that the best amount of exergy efficiency is 40 %.

In this study, by engine thermodynamic modeling CFM56 3B2 and F119 PW100, the effect of inlet air temperature on performance of the turbofan engine and optimizing the performance of the turbofan engine in take-off condition M=0, H=0 and design condition M=0.85, H=10000m have been investigated. This modeling is done in GASTURBINE10 software. First, the effect of the inlet air temperature on the performance of the turbofan engine was investigated. Four types of hydrogen fuel, natural gas JP4 and JP10 are considered. Optimization for both GENX 1B70 and CFM56 3B2 engines is done by using hydrogen fuel.The objective functions of the parameters that indicate the performance of the motor turbofan, such as thrust force, TSFC, thermal efficiency and output snox, turbine inlet temperature, Engine inlet air temperature with ambient air temperature difference, compressor pressure ratio and fan pressure ratio, bypass ratio are considered as design variables.The results of the optimization based on the four objective functions for take-off condition M=0,H=0 and design condition M=0.85,H=10000 have been compared with the reference values for each engine. The TOPSIS algorithm has been used to select the best condition from the optimized conditions for both environmental and economic approaches.

Problem Description

The gas turbine is an internal combustion engine, one of the most prominent examples of which is the aircraft engine. The inlet air to the engine is heated and compressed in a hot compressor. Then, in the fuel combustion chamber, it reacts ideally in a steady-state pressure process. The hot and dense gases from the combustion of the turbine are moved and then discharged through the nozzle to the ambient. The axial power generated in the turbine supplies the compressor power consumption, due to the difference in velocity of the output current from the nozzle relative to the speed of the air entering the engine. The other term of the thrust force is generated by the difference in output current pressure with the ambient pressure. Gas turbine engines operate on the Brayton cycle. The main parts of the cycle include the compressor, combustion chamber, turbine, and nozzle. The design of gas turbine engines is very complex and begins with thermodynamics cycle analysis. Its main parameters include compression ratio, turbine inlet temperature, and bypass ratio. Optimizing these parameters is very important for purposes such as increasing thrust and reducing specific consumption (TSFC). Turbojet engines are one of the simplest configurations of aero gas turbine engines. Turbojet engines are divided into two categories: single spool and twin spool. In single-spool gas turbine engines, the shaft connects the compressor power to the turbine. Dual-spool type includes the high-pressure compressor, low-pressure compressor, low-pressure turbine, high-pressure turbine, low-pressure turbine, and combustion chamber. In this configuration, the high-pressure spool connects the high-pressure spool to the high-pressure compressor and the low-pressure spool connects the low-pressure compressor to the low-pressure turbine. Another type of gas turbine engine that was studied in this study is the turbofan engine. In these engines, the engine's internal flow is divided into two parts: hot flow and bypass flow. These engines combine turbojet as hot core and bypass flow as cold flow. Turbofan engines are divided into two types, twin-spool, and three spools. Twin spool turbofan includes a low-pressure compressor and high-pressure compressor, high-pressure turbine fan, low The high pressure to the high-pressure turbine and the low-pressure shaft connects the low-pressure turbine to the low-pressure compressor and fan. It then moves the hot, dense gases from the turbine combustion and then

discharges them into the ambient through the nozzle. The axial power generated in the turbine supplies the compressor power consumption, due to the difference in velocity of the output current from the nozzle relative to the inlet air velocity of one term of the thrust force. The other semester of the thrust force is produced by the difference between the outlet pressure and the ambient pressure.[10]

Three-spool turbofan includes high-pressure, low-pressure, medium-pressure, high-pressure turbine, medium-pressure, low-pressure, combustion chamber, and nozzle fan. In these engines, the high-pressure shaft connects the high-pressure compressor to the high-pressure turbine. Medium pressure compressor is connected to medium pressure turbine by medium pressure shaft. The low-pressure shaft connects the low-pressure turbine to the fan. Turbofan engines are also divided into two categories: mixed flow turbofan and unmixed flow turbofan. In turbofan engines, the cold flow and hot flow mixes are mixed before entering the nozzle in the mixer and then entering a nozzle. In unmixed flow turbofan engines, the cold flow is discharged from the unique nozzle and the hot flow is discharged from the unique nozzle to the environment.[11]

In order to add a cooling system to the engine system, it is recommended to use the engine intake duct as a cooling converter.

In this study thermodynamic modeling, CFM56 3B2, and F119 PW100 engine cycles are done with GASTURB 10 software. First, the effect of the inlet air temperature on the performance of the turbofan engines was investigated.

A schematic of a mixed flow turbofan engine with an inlet air cooling system and an unmixed flow turbofan engine with an inlet air cooling system is shown in Fig. 1.

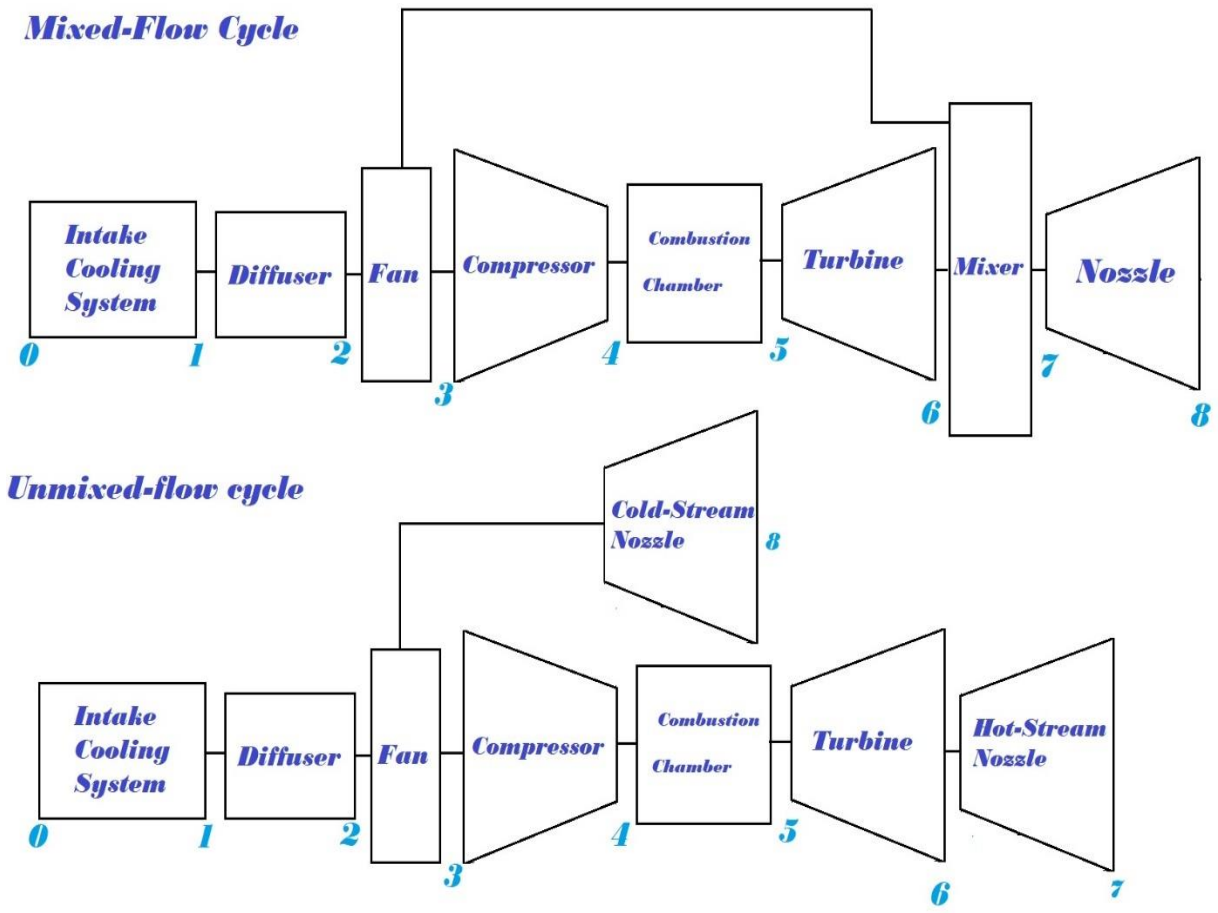

Figure 1. turbofan engine cycle with inlet air cooling system flow diagram.

A schematic of mixed flow twin spools turbofan engine and an unmixed flow twin spools turbofan engine is shown in Fig. 2.[12]

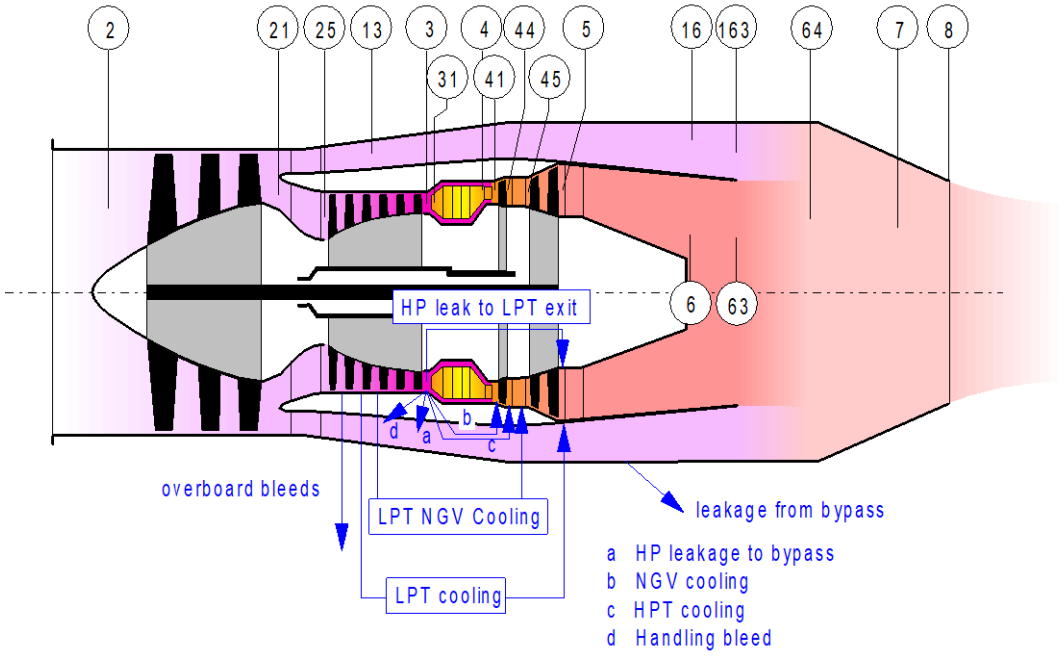

a)

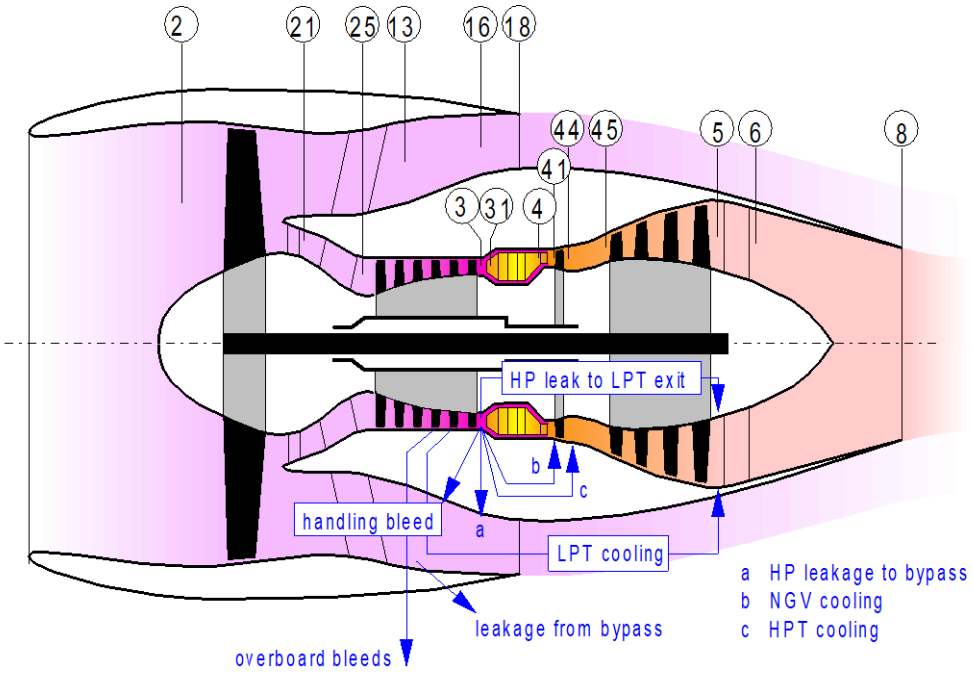

b)

Figure 2. a) mixed flow turbofan schematic **b)** unmixed flow turbofan schematic

The changes in airflow pressure at the intake and cooling system are negligible, so the governing equation can be calculated.

Table 1 showed the temperature and pressure at each state.

Table 1. Temperature and pressure of each state

State	***Pressure***	***Temperature***
1	$\boldsymbol{P_1 = P_0}$	$\boldsymbol{T_1 = T_0 + \Delta T}$
2	$\boldsymbol{P_2 = P_1\left(\frac{T_2}{T_1}\right)^{\frac{k_d}{k_d-1}}}$	$\boldsymbol{T_2 = T_1\left(1 + \frac{k_d - 1}{2} M_a^2\right)}$
3	$\boldsymbol{P_{3=\pi_{fan}} P_2}$	$\boldsymbol{T_3 = \frac{T_2}{\eta_{fan}}\left[\left(\frac{P_3}{P_2}\right)^{\frac{k_f-1}{k_f}} - 1\right] + T_2}$
4	$\boldsymbol{P_{4=\pi_c} P_3}$	$\boldsymbol{T_4 = \frac{T_3}{\eta_C}\left[\left(\frac{P_4}{P_3}\right)^{\frac{k_c-1}{k_c}} - 1\right] + T_3}$
5	$\boldsymbol{P_5 = P_4 - \Delta P_{CC}}$	$\boldsymbol{T_5 = \frac{P_4 - \Delta P_{CC}}{R}}$
6	$\boldsymbol{P_6 = P_5\left[1 - \frac{1}{\eta_t}\left(1 - \frac{T_6}{T_5}\right)\right]^{\frac{k_t}{k_t-1}}}$	$\boldsymbol{T_6 = \frac{P_5\left[1 - \frac{1}{\eta_t}\left(1 - \frac{T_6}{T_5}\right)\right]^{\frac{k_t}{k_t-1}}}{R}}$
7	$\boldsymbol{P_7 = P_6\left[1 - \frac{1}{\eta_{nh}}\left(1 - \left(\frac{T_7}{T_6}\right)\right)\right]^{\frac{K_{nh}}{K_{nh}-1}}}$	$\boldsymbol{T_7 = \frac{T_6 C_{P6} m_{ah} + (m_{ac} C_{P3} T_3)}{C_{P7}}}$
8 mixed	$\boldsymbol{P_{8,mi} = P_3\left[1 - \frac{1}{\eta_{nc}}\left(1 - \left(\frac{T_8}{T_3}\right)\right)\right]^{\frac{K_{nc}}{K_{nc}-1}}}$	$\boldsymbol{T_{8,mi} = \frac{P_3\left[1 - \frac{1}{\eta_{nc}}\left(1 - \left(\frac{T_8}{T_3}\right)\right)\right]^{\frac{K_{nc}}{K_{nc}-1}}}{R}}$
8 unmixed	$\boldsymbol{P_{8,un} = P_7\left[1 - \frac{1}{\eta_n}\left(1 - \left(\frac{T_8}{T_7}\right)\right)\right]^{\frac{K_n}{K_n-1}}}$	$\boldsymbol{T_{8,un} = \frac{P_7\left[1 - \frac{1}{\eta_n}\left(1 - \left(\frac{T_8}{T_7}\right)\right)\right]^{\frac{K_n}{K_n-1}}}{R}}$

The performance parameters can be calculated as the function of temperature, pressure and flight speed.

First, thrust force of the mixed-flow engine is calculated in such a way;

$$F_{mi} = m_7(V_8 - V_0) + A_8(P_8 - P_0) \quad (1)$$

where P_0, V_0, A_8 and m_7 respectively is the ambient pressure and flight speed, the area of the nozzle output section, and the mixer exit mass flow rate.

The thrust force of unmixed-flow engine is divided in two sections: hot stream nozzle thrust and cold stream nozzle thrust.

The hot stream nozzle thrust is calculated as;

$$F_{hot} = \frac{1}{g_c}\left[\left((m_{ah} + m_f)(V_7)\right) - (m_{ah}V_0)\right] + [A_7(P_7 - P_0)] \quad (2)$$

where A_7, P_0, V_0, g_c, and m_{ah} are the hot stream nozzle exit area, the ambient air pressure, the flight speed, and is the gravity of the earth, cold stream real mass flow rate, and the hot stream real air mass flow rate, respectively.

The cold stream nozzle thrust is calculated as;

$$F_{cold} = \frac{1}{g_c}\left[\left((m_{ac})(V_8)\right) - (m_{ac}V_0)\right] + [A_8(P_8 - P_0)] \quad (3)$$

whereA_8, V_8 and P_8 are the cold flow nozzle exit area, the cold flow nozzle exit speed and the pressure at the cold nozzle output.

The total thrust of unmixed-flow engine is calculated as;

$$F_{un} = F_{hot} + F_{cold} \quad (4)$$

Second, the other performance parameters can be determined also as the function of temperature, pressure, flight speed, and mass flow rate.

The other performance can be illustrated at table 2.

Table 2. performance parameters

Symbol	***Description***	***Calculation***
$TSFC$	Thrust Specific fuel Consumption	$\frac{m_f}{F_{tot}}$
η_{th}, mi	Thermal efficiency of mixed-flow engine	$\frac{m_7(V_8^2 - V_0^2)}{2m_f FHV}$
η_{th}, un	Thermal efficiency of unmixed-flow engine	$\frac{\left[(m_{ah} + m_f){V_7}^2 - \left(m_{ah}{V_0}^2\right) + m_{ac}\left({V_8}^2 - {V_0}^2\right)\right]}{2m_f FHV}$
$\eta_{P,mi}$	Propulsive efficiency of mixed-flow engine	$\frac{V_0 F_{mi}}{m_7(V_8^2 - V_0^2)}$
$\eta_{p,un}$	Propulsive efficiency of unmixed-flow engine	$\frac{F_{un}V_0}{\left[(m_{ah} + m_f){V_7}^2 - \left(m_{ah}{V_0}^2\right) + m_{ac}\left({V_8}^2 - {V_0}^2\right)\right]}$
TSF	Specific thrust force	$\frac{F_{tot}}{m_{tot}}$
S_{NOx}	The nitrate oxide emission index coefficient	$\left(\frac{P_4}{2965kPa}\right)^{0.4} e^{\left(\frac{T_4 - 826K}{194K} + \frac{6.29 - (100.war)}{53.2}\right)}$

where F_{tot} is total thrust force, it depends on type of engine, for mixed-flow engine is $F_{tot} = F_{mi}$ and for unmixed-flow engine is $F_{tot} = F_{un}$, also war and FHV are compression ratio and fuel heat value, $m_{tot}$is intake engine mass fliw rate that can be calculated as follows;

$$m_{tot} = m_{ac} + m_{ah} \quad (5)$$

CFM56 3B2

The main components of this engine include a one-stage axial fan, three stages low-pressure axial flow compressor, nine-stage high axial flow pressure compressor, annular combustion chamber, one-stage high-pressure axial flow turbine, and four-stage low-pressure axial flow turbine. The length of the engine is 236.7 mm, its diameter is 201.8mm, and its dry weight is 1955kg. The engine has been used as a propulsion system for aircraft such as airbus 320 and Boeing 737.[13]

F119 PW100

The main components of this engine include a three-stage axial flow fan, a six-stage axial flow compressor, an annular combustion chamber, a one-stage high-pressure axial flow turbine, and a one-stage low-pressure axial flow turbine. This engine has been used as a propulsion system for the F22 RAPTOR aircraft produced by the LOCKHEED MARTIN company.[22] This engine has afterburner capability, but in this study, the state without afterburner was considered for it. The input parameters for all three engines are given in Table 3.

Table 3. the input parameters for all three engines.[13]

	CFM 56 3B2	**F119 PW100**
$T_{inlet\ turbine}$	1600(K)	1920(K)
$r_{p,compressor}$	24.11	35
$r_{p,fan}$	1.655	4
$Bypass\ ratio$	4.9	0.45
$\dot{m}_{air}$	313.798(Kg/s)	122(Kg/s)
$\eta_{is,fan}$	0.90	0.91
$\eta_{is,compressor}$	0.87	0.91

The effect of several types has been investigated on the performance of the both CFM56 3B2 and F119 PW100 engines.

The considered fuels are hydrogen fuel, natural gas, JP4, and JP10.

The fuel thermal value (FHV) is given for each fuels in Table 2.[1]

Table 2. fuel thermal value (FHV) for considered fuel

Fuel type	**hydrogen**	**Natural gas**	**JP4**	**JP10**
FHV	118(MJ/kg)	49.736(MJ/kg)	43.323(MJ/kg)	42.076(MJ/Kg)

Decreasing the inlet air temperature drop increases the air density and increases the inlet air real mass flow rate as the air density increases. Increasing the flow of air entering the engine increases the term due to the difference in thrust force. It has also been observed; whatever, fuel molecular weight be less, the molecular weight of fuel combustion productions with air is less too. As the molecular weight of the combustion

productions decreases, the rate of emission from the nozzle increases. As a result, the thrust force of the thrust force increases. Therefore, the thermodynamic cycle has the highest thrust force per hydrogen fuel. Thrust force changes with changes in inlet air temperature with take-off condition for CFM56 3B2 and F119 PW100 engines are shown in Fig.5.

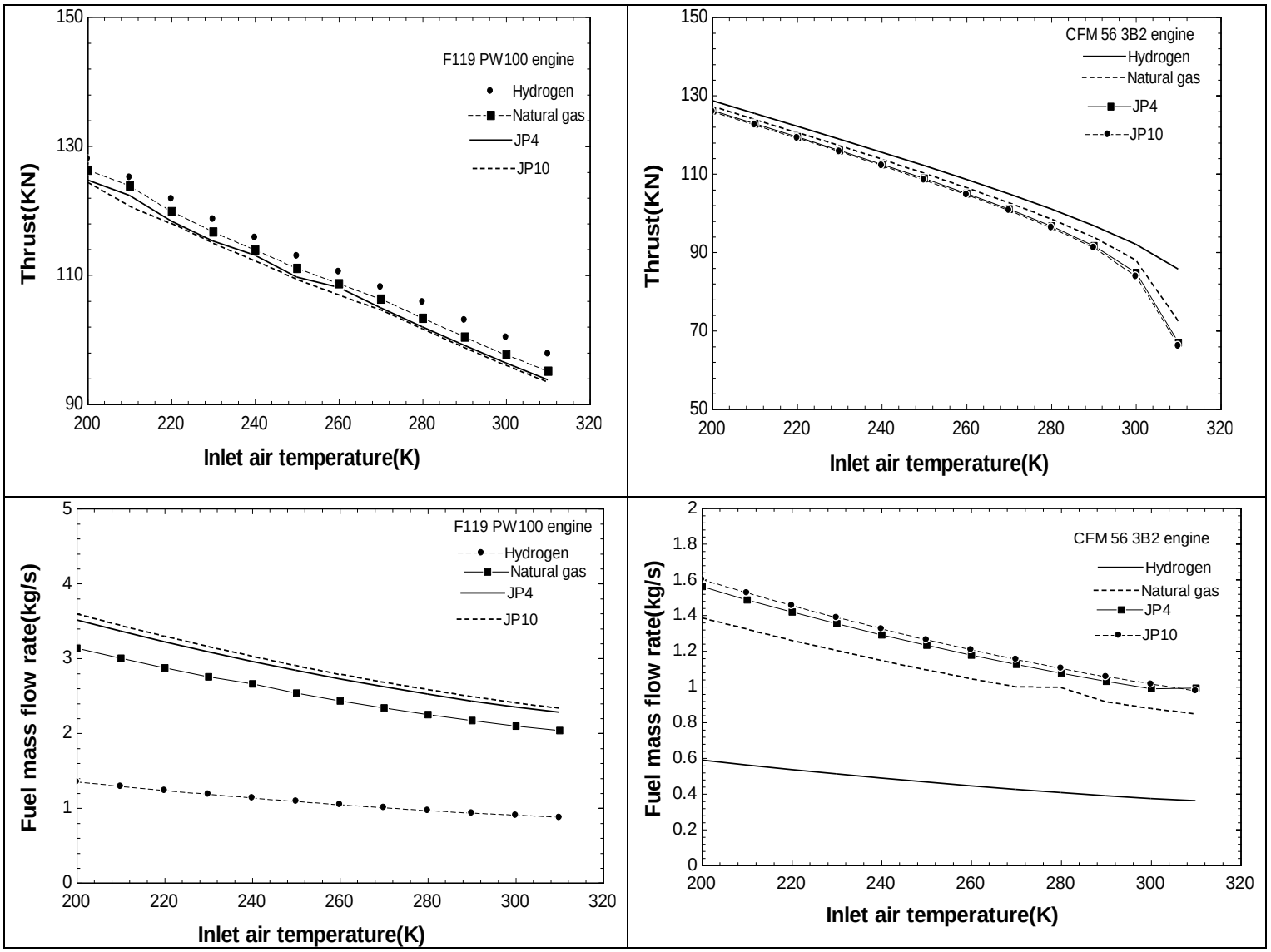

Figure.5. Thrust force changes with changes in inlet air temperature with take-off condition for CFM56 3B2 and F119 PW100 engines

Figure.6. The engines fuel flow rate changes with inlet air temperature in the take-off condition M=0, H=0 for the CFM56 3B2 and F119 PW100 engines

The engines fuel flow rate changes with inlet air temperature in the take-off condition M=0, H=0 for the CFM56 3B2 and F119 PW100 engines are shown in fig.6.

As a result, the drop of inlet air temperature under equal conditions, higher heat is required to bring the temperature of each kilogram of inlet air to the inlet air temperature of the turbine. With drop of inlet air temperature, real inlet air mass flow rate also increases; as a result, fuel mass flow rate increases. It has also

been observed that as fuel heat value (FHV) increases, fuel mass flow rate decreases because heat rate is constant under equal conditions. Therefore, thermodynamic cycle for hydrogen fuel has the lowest fuel mass flow rate compared to other fuels. 70 Engine thermal efficiency changes with inlet air temperature changes with take-off condition (M = 0, H = 0) for CFM56 3B2 and F119 PW100 engines in Fig.7 shows.

The real inlet air mass flow rate is greater than the increase in fuel mass flow rate. Therefore, with decreasing inlet air temperature drop, the thermal efficiency of the cycle increases. Also, because the changes in the temperature of inlet air the engine are not dependent on the type of fuel, and by increasing the heat value of the fuel in the condition equal, fuel mass flow rate decreases. As a result, less heat is required to raise the flow temperature to the inlet air temperature of the turbine.as a result, thermal efficiency increases with decreasing heat rate and increasing heat value.Fig.8 shows Fuel consumption changes (TSFC) for inlet air mass flow rate changes in take-off condition (M = 0, H = 0) for CFM56 3B and F119 PW100 engines.

It is observed that in order to reduce the inlet air temperature drop in the temperature range of less than 290 K, the thrust force is less than the rate of increase of the fuel mass flow rate. Therefore, the specific fuel consumption (TSFC) increases. Also, since the heat rate is stable under equal condition, TSFC decreases with increasing value of fuel heat, so hydrogen has the lowest TSFC. Changes in SNOx with inlet air temperature changes according to Kelvin in take-off condition (M = 0, H = 0) (take off condition) for CFM56 3B2 and F119 PW100 engines are shown in Fig.9.

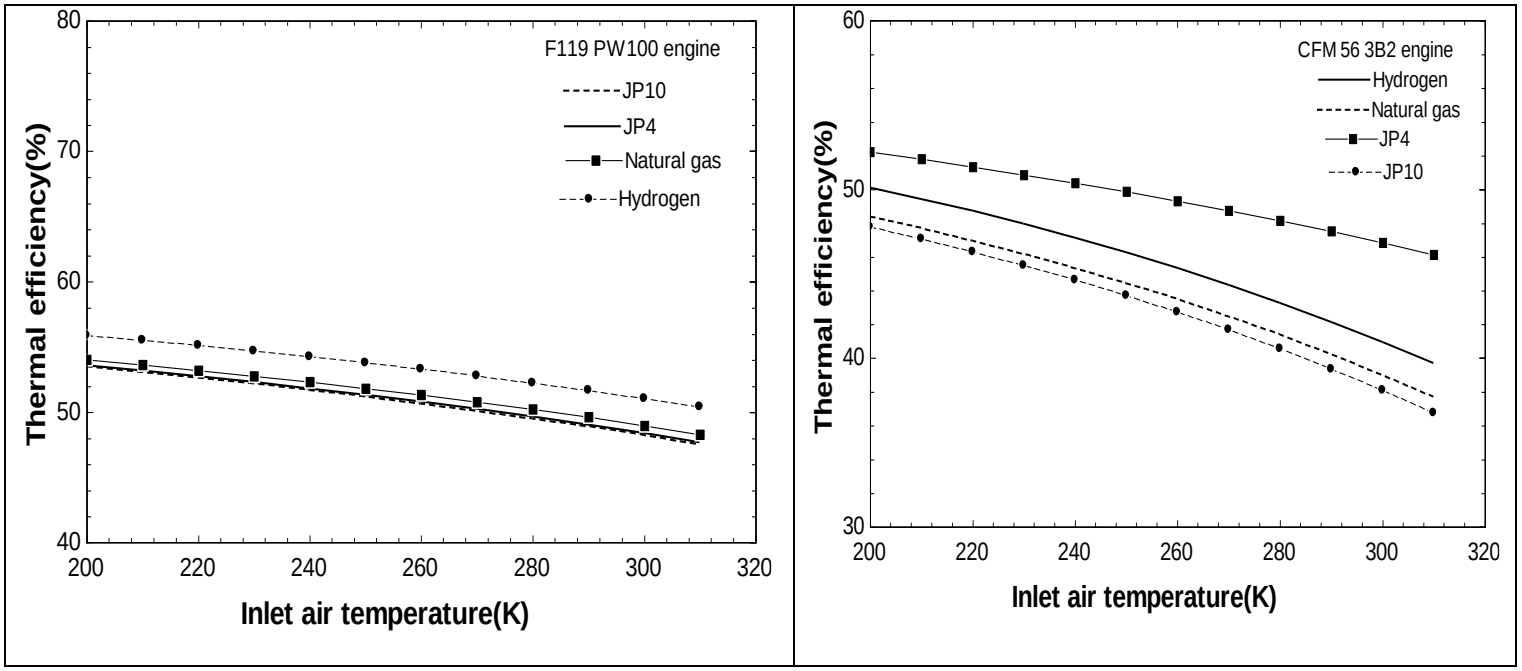

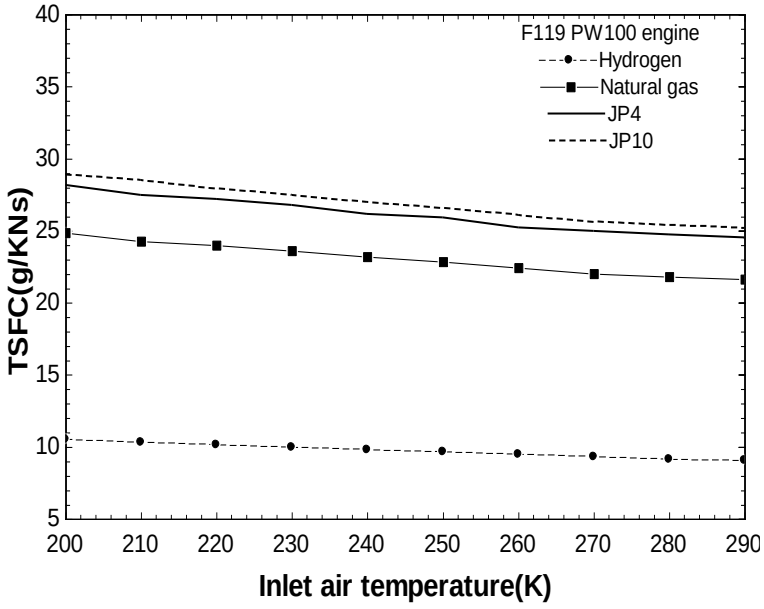

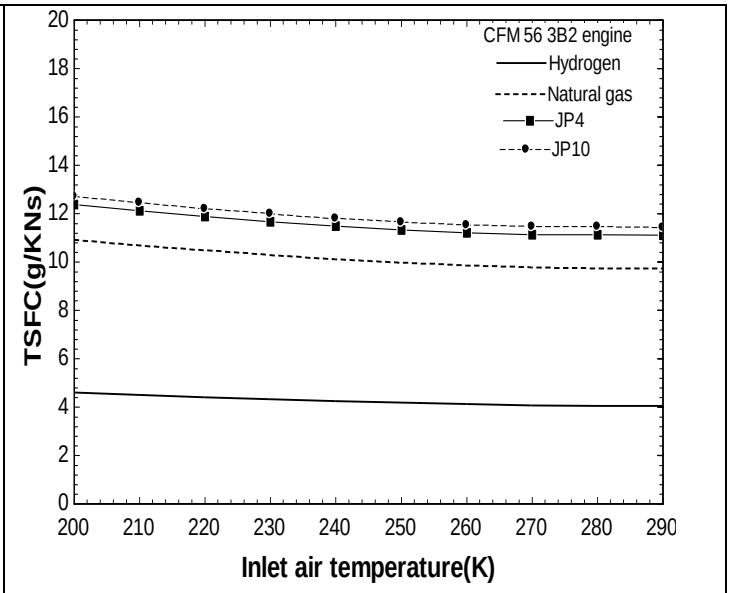

Figure.7. thermal efficiency changes with inlet air temperature changes with take-off condition (M = 0, H = 0) for CFM56 3B2 and F119 PW100 engines

Figure.8. Fuel consumption changes (TSFC) for inlet air mass flow rate changes in take-off condition (M = 0, H = 0) for CFM56 3B2 and F119 PW100 engines.

1. Kurzke, J., Gasturb 11, User Manual. 2007, June.

In this study CFM56 3B2 engines were optimized. To optimization these engines, 4 separate objective functions were used and a separate optimization was performed for each target area. These objective functions include 1-thrust force maximize 2-thermal efficiency maximize 3-TSFC minimization 4-snox minimize. According to studies, thrust force of the thermodynamic cycle is the maximum for liquid hydrogen fuel.it also has the highest thermal efficiency but lowest TSFC compared to other fuels studied in the same condition, so it was selected to optimize hydrogen fuel. The design variables and their ranges are shown in Table 4.

Table 4. The design variables and their ranges for CFM56 3B2 engines.

engine		$T_{inlet\ turbine}$	ΔT	$r_{p,fan}$	$r_{p,comperssor}$	$Bypass\ ratio$
	lower bound	1000	-40	1.05	12	0.1
CFM56 3B2	upper bound	1950	10	4	25	15

For optimization of CFM56 3B2 engine. Optimization constrains based on the objective function for CFM56 3B2 engines are given in Tables 5 and 6.

Tables 6. Optimization constrains based on the objective function for CFM56 3B2 engine

Objective function	PARAMETER	MINIMUM VALUE	MAXIMUM VALUE
$snox$	$TSF(Ns/Kg)$	330	400

	$TSFC(g/KNs)$	2	4.14
$TSFC(g/KNs)$	$\eta_{thermal}(\%)$	40	55
	$Thrust(KN)$	100	200
$\eta_{thermal}(\%)$	$TSFC(g/KNs)$	2	4.14
	$Thrust(KN)$	100	200
$Thrust(KN)$	$TSFC(g/KNs)$	2	4.14

Optimization was performed using genetic algorithm and according to design variable ranges, optimization constrain and objective functions and by using genetic algorithm. The optimal design parameters for both engines are shown in Table 7.

Table 7. The optimal design parameters for both engines

engine	$objective\ function$	$T_{inlet\ turbine}$	ΔT	$r_{p,fan}$	$r_{p,comperssor}$	$Bypass\ ratio$
CFM56 3B2	$Thrust$	1940.53	-39.98	2.36	24.99	7.14
	$\eta_{thermal}$	1949.8	-39.99	2.02	24.99	7.7
	$TSFC$	1916.32	-39.99	1.75	24.99	11.61
	$snox$	1714.83	-39.99	1.93	14.19	7.06

The results of the optimization have been compared with the results of the basic line engine cycles for hydrogen fuel in the take-off condition H=0, Mach=0 and design condition, for GENX 1B70 and CFM56 3B2 are given in tables 8 and 9.

Table 8. The results of the optimization have been compared with the results of the basic line engine cycles for hydrogen fuel for CFM56 3B2 engine

base on objective function	$\dot{m}_{air}(\frac{kg}{s})$	$\dot{m}_{fuel}\left(\frac{kg}{s}\right)$	$Snox$	$\eta_{thermal}$	$TSFC(\frac{g}{KNs})$	$Thrust(KN)$
$IN\ TAKE\ OFF\ CONDITION$[23]	310.065	0.423	0.721	43.52	4.136	102.49
$Thrust$	334.72	0.533	0.463	49.25	4.139	128.99
$\eta_{thermal}$	334.733	0.504	0.463	49.26	4.092	123.26
$TSFC$	334.724	0.336	0.463	49.14	3.363	100.01
$snox$	334.724	0.457	0.22	43.2	4.139	110.54
$ON\ DESIGN\ CONDITION$[23]	138.097	0.203	0.342	52.98	7.519	27.12
$Thrust$	152.453	0.26	0.196	56.79	7.02	37.04
$\eta_{thermal}$	152.46	0.245	0.196	56.78	7.258	33.83
$TSFC$	152.458	0.164	0.196	56.7	6.462	25.38
$snox$	152.458	0.222	0.1	51.42	7.278	30.53

Relative changes in thrust force, specific consumption (TSFC), thermal efficiency, SNOx, fuel mass flow rate and real inlet air mass flow rate in optimal condition Based on thrust force maximization, thrust force, special consumption (TSFC), thermal efficiency, SNOx, fuel mass flow rate and real air flow The inlet air mass flow rate for the take-off mode for commercial GENX 1B70 engine and for commercial CFM56 3B2 engine is shown in Tables 10 and 11, respectively.

Table 11 Tables 10 Relative changes in thrust force, specific consumption (TSFC), thermal efficiency, SNOx, fuel mass flow rate and real inlet air mass flow rate in optimal state for commercial CFM56 3B2 engine

base on objective function		$\dot{m}_{air}$	$\dot{m}_{fuel}$	$Snox$	$\eta_{thermal}$	$TSFC$	$Thrust$
$Thrust$	$IN\ TAKE\ OFF\ CONDITION$[24]	7.952	26.0	-35.8	13.2	0.1	25.9
$\eta_{thermal}$		7.956	19.1	-35.8	13.2	-1.1	20.3
$TSFC$		7.953	-20.6	-35.8	12.9	-18.7	-2.4
$snox$		7.953	8.0	-69.5	-0.7	0.1	7.9
$Thrust$	$ON\ DESIGN\ CONDITION$[24]	10.396	28.1	-42.7	7.2	-6.6	36.6
$\eta_{thermal}$		10.401	20.7	-42.7	7.2	-3.5	24.7
$TSFC$		10.399	-19.2	-42.7	7.0	-14.1	-6.4
$snox$		10.399	9.4	-70.8	-2.9	-3.2	12.6

It is observed the optimization of SNOx production based on the target function has increased to 0.2% compared to the take-off condition of the GENX 1B70 engine, and optimization has decreased in other condition of the take-off condition and design condition. The thermal efficiency is reduced by only 0.3% in the state of optimization is based on the target function of TSFC and compared to the design condition in the GENX 1B70 engine. There is a decrease compared to both take off condition and design condition. The real inlet air mass flow rate in the optimal conditions for the engine have been few changes compared to the take-off condition and design condition.

It can be seen that the changes on design conditions and take off conditions of both engines are different by using the optimal values of the design variables. Therefore, because the performance of the motors is different for each objective function and the decision is a bit difficult. Using the TOPSIS algorithm, the optimization results are prioritized based on two environmental and economic approaches.

Since most of the performance of the engines is on the design point condition there are 4 indicators for choosing the optimal cycle, thrust, thermal efficiency for fuel consumption (TSFC) And the index of nitric oxide intensity produced in the design point design condition (M = 0.85, H = 10000m) was considered in this optimization. For all four indicators in both approaches, weight coefficients are considered (Table 12).

Table 12. weight coefficients for environment and economic approaches in TOPSIS algorithm

	$Thrust$	$\eta_{thermal}$	$TSFC$	$snox$
Environment approach	0.85	0.9	-0.95	-1
Economic approach	0.85	0.95	-1	-0.9

The results of decision-making with the environmental or environmental approach and the economic approach are shown in Fig.11.

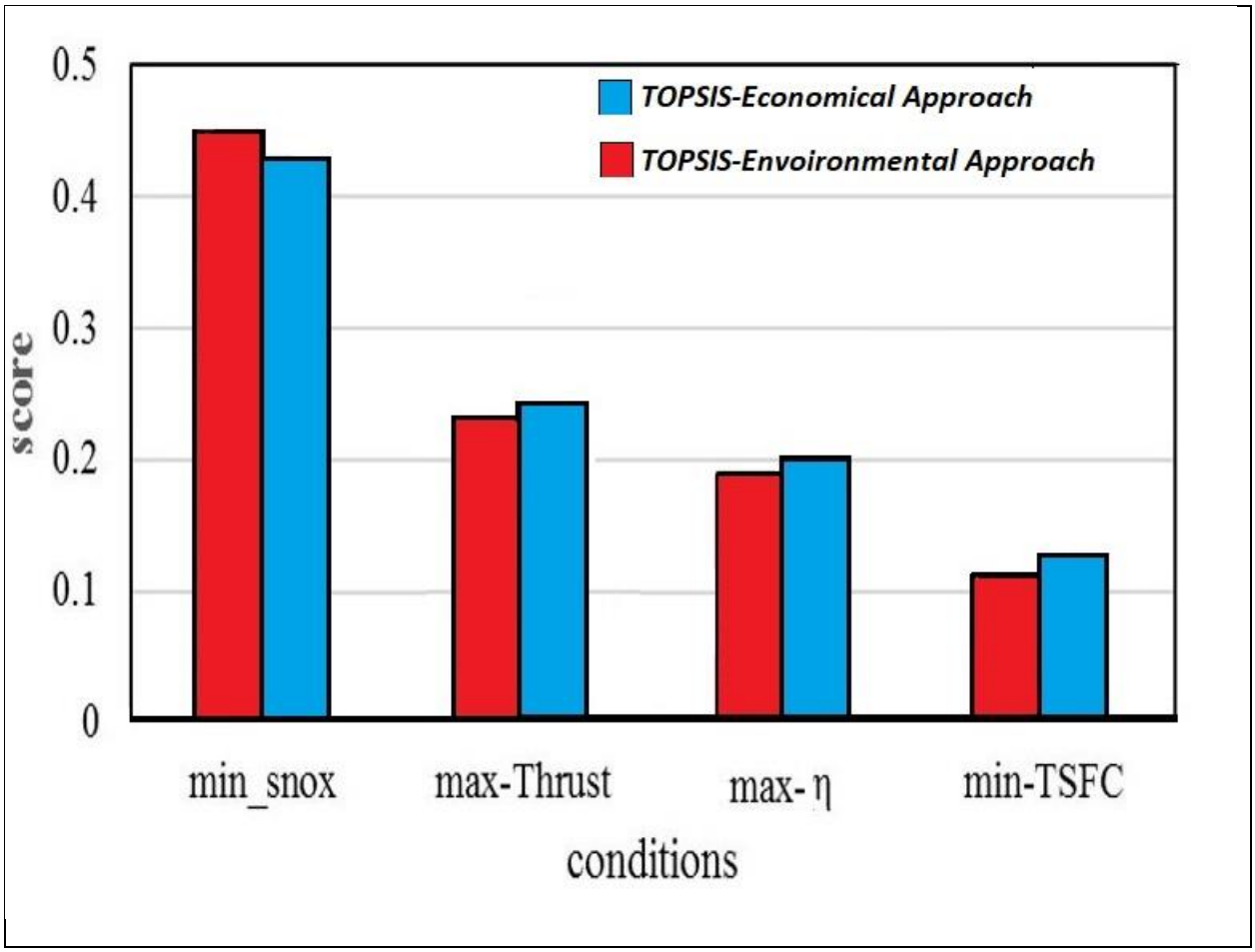

Figure 11. The results of decision-making

Therefore, the optimized cycle was selected for the minimization of the SNOx minimize for the environmental approach from among the optimized cycles based on the CFM56 3B2-cycle. It is observed in the environmental approach, the performance of the engines in minimizing the amount of SNOx has the highest score and in minimizing TSFC has lowest score for both engines. Also, in the economic approach, the highest score is for optimization of SNOx target function and lowest score belongs to the optimization of TSFC target function. The temperature–entropy diagram of optimized cycle for parameter of minimization for CFM56 3B2 engines are shown in Fig.12.

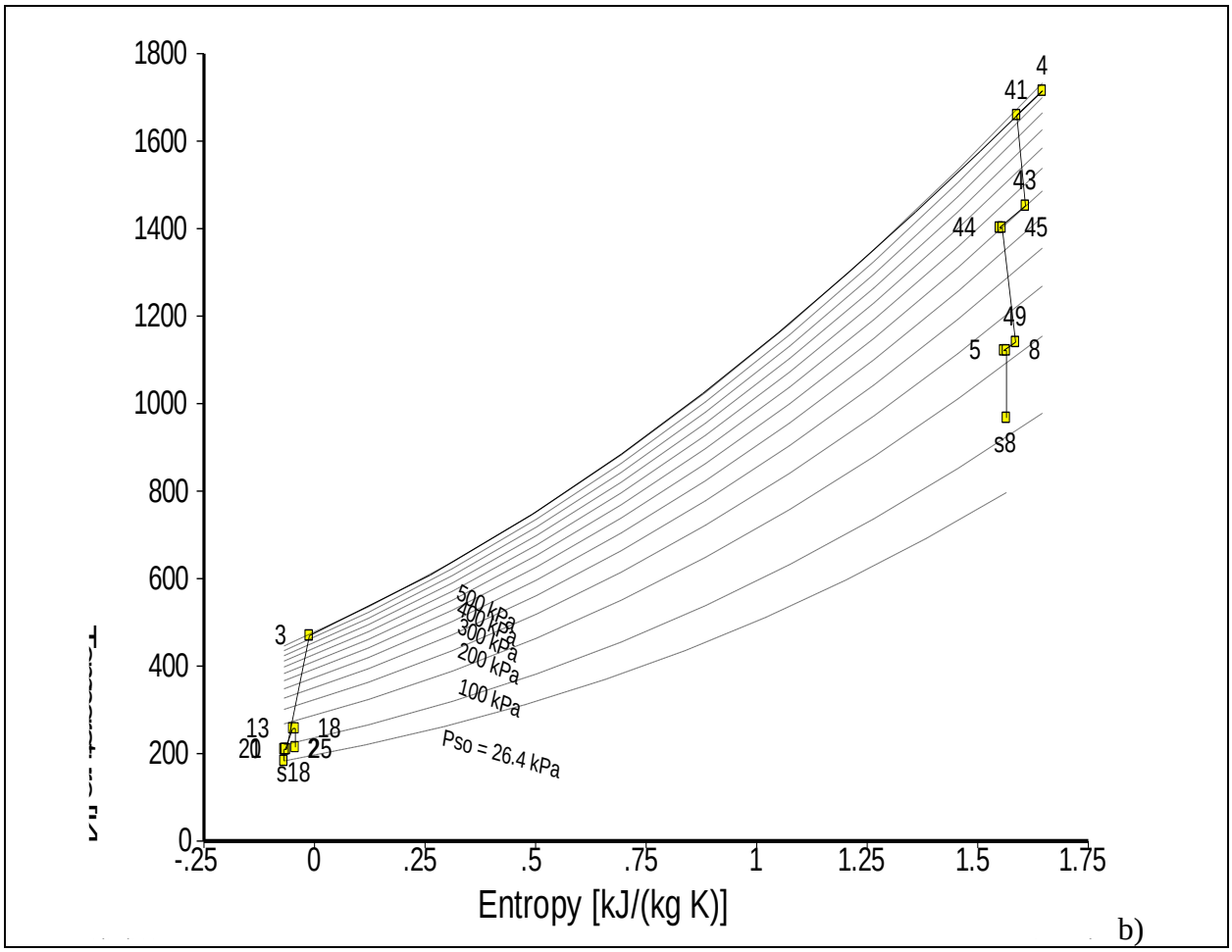

Figure.12. The temperature – entropy diagram of optimized cycle for parameter of minimization for CFM56 3B2 engines

Conclusions

In this study, modeling of CFM56 3B2,F119PW100 engines to investigate the effect of inlet air temperature on turbofan engine performance and turbofan engine performance optimization in take-off condition. This modeling is done with GASTURB 10 software. First effect of inlet air cooling on turbofan engines was examined. Results show that for four type of fuels liquid hydrogen, liquid natural gas,JP4 and JP10 with inlet air temperature drop thrust, TSFC, thermal efficiency, inlet air mass flow rate, fuel mass flow rate increase and snox decreases. Optimization was performed for both GENX 1B70 CFM56 3B2 engines by using hydrogen fuel. The target functions are parameters that represent the performance of the turbofan engine, such as thrust, TSFC, thermal efficiency, and the amount of snox. The inlet temperature of turbine, the difference between inlet air temperature the engine and ambient air temperature, the compression ratio in the compressor and in the fan, and bypass ratio are considered as design variable. The results of optimization based on the four objective functions for both conditions were compared with the reference values for each engine for examples include thrust maximization, thrust force, TSFC, thermal efficiency, snox, and fuel mass. flow rate) and the real air mass flow rate relative to the take-off condition of the GENX 1B70 engine (about 55.2%, 20%, 6.14%, 20.26%, 86.7% and 6.45%)And for the engine CFM56 3B2 it has changed by about 25.8%, 0.072%, 13.16%, 35% -, 26% and 7.95%. These changes are different based on the optimization with the four objective functions mentioned, so the TOPSIS algorithm is used.

Considering the thrust force, thermal efficiency, TSFC, and production snox as a criterion and determination of weight coefficients based on two economic and environmental perspective, the desired conditions have been prioritized. For both engines and both approaches by using the TOPSIS algorithm, the highest score for the optimization mode with the snox function and the lowest score belong to the optimization mode based on the target function of the TSFC. Thrust power has been increased by about 19.1 % and 12.6% based on optimization with snox function compared based on design condition for GENX 1B70 and CFM56 3B2 engines.

References

1. Turan, O., *Exergetic effects of some design parameters on the small turbojet engine for unmanned air vehicle applications.* Energy, 2012. **46**(1): p. 51-61.
2. S.H. Najjar, Y. and I. A.I. Balawneh, *Optimization of gas turbines for sustainable turbojet propulsion.* Propulsion and Power Research, 2015. **4**(2): p. 114-121.
3. Seyam, S., I. Dincer, and M. Agelin-Chaab, *Novel hybrid aircraft propulsion systems using hydrogen, methane, methanol, ethanol and dimethyl ether as alternative fuels.* Energy Conversion and Management, 2021. **238**: p. 114172.
4. Nordin, A., et al. *Turbine Inlet Air Cooling for Industrial and Aero-derivative Gas Turbine in Malaysia Climate*. in *IOP conference series: Earth and environmental science*. 2017. IOP Publishing.
5. Tang, H.-L., et al., *High altitude low Reynolds number effect on the matching performance of a turbofan engine.* Proceedings of the Institution of Mechanical Engineers, Part G: Journal of Aerospace Engineering, 2012. **227**(3): p. 455-466.
6. Zare, V., *Performance improvement of biomass-fueled closed cycle gas turbine via compressor inlet cooling using absorption refrigeration; thermoeconomic analysis and multi-objective optimization.* Energy Conversion and Management, 2020. **215**: p. 112946.
7. Tuzcu, H., Y. Sohret, and H. Caliskan, *Energy, environment and enviroeconomic analyses and assessments of the turbofan engine used in aviation industry.* Environmental Progress & Sustainable Energy, 2020: p. e13547.
8. Patel, V., V. Savsani, and A. Mudgal, *Efficiency, thrust, and fuel consumption optimization of a subsonic/sonic turbojet engine.* Energy, 2018. **144**: p. 992-1002.
9. Najjar, Y. and A. Abubaker, *Thermoeconomic analysis and optimization of a novel inlet air cooling system with gas turbine engines using cascaded waste-heat recovery.* Energy, 2017. **128**.
10. Mattingly, J.D., K.M. Boyer, and H. von Ohain, *Elements of propulsion: gas turbines and rockets*. 2006: American Institute of Aeronautics and Astronautics Reston, VA.
11. El-Sayed, A.F., *Fundamentals of aircraft and rocket propulsion*. 2016: Springer.
12. *GasTurb GmbH, 2021, "GasTurb 13 Manual: Design and Off-Design Performance of Gas Turbines," GasTurb GmbH, Aachen, Germany, accessed April 21, 2021 from https://www.gasturb.de/download.html#user-manuals.*

13. Martins, D.A.R., *Off-design performance prediction of the cfm56-3 aircraft engine.* Tecnico Lisboa MSc Thesis, 2015.